Journal of Anatomy

J. Anat. (2010) **216**, pp671–682 doi: 10.1111/j.1469-7580.2010.01229.x

Fetal anatomy of peripheral lymphatic vessels: a D2-40 immunohistochemical study using an 18-week human fetus (CRL 155 mm)

Zhe Wu Jin,[1] Takuo Nakamura,[2] Hee Chul Yu,[1] Wataru Kimura,[3] Gen Murakami[4] and Baik Hwan Cho[1]

[1]*Department of Surgery and Research Institute of Clinical Medicine, Chonbuk National University Medical School, Jeonju, Korea*
[2]*Department of Physical Therapy, Sapporo Medical University School of Health Science, Sapporo, Japan*
[3]*Department of Gastroenterologic Surgery, Yamagata University School of Medicine, Yamagata, Japan*
[4]*Division of Internal Medicine, Iwamizawa Koujin-kai Hospital, Iwamizawa, Japan*

Abstract

We demonstrated fetal peripheral lymphatic vessels (LVs) using D2-40 immunohistochemistry in a whole female fetus (18 weeks of gestation, CRL 155 mm) except for the head. There were abundant LVs in the thyroid gland, lung, stomach, small intestine, rectum and pancreas, whereas no LVs were seen in the parathyroid gland, spleen and adrenal cortex. In the liver, except for the gallbladder bed, LVs were still restricted to around hilar thick portal veins and around the hepatic vein terminals. Subcutaneous LVs were well developed throughout the body even in areas where no or few perforating LVs connected with the deep LVs. The diaphragm contained abundant, dilated LVs in the pleural half of its thickness. LVs were also seen not only along supplying arteries of muscles and cartilage but also along the epimysium and perichondrium. LVs ran in a space between the obliquus internus and transversus abdominis but not between the obliquus internus and obliquus externus. Some tight connective tissues such as the sacrotuberous ligament contained abundant LVs. The intervertebral foramen contained a lymphatic plexus. The present observations provide a better understanding of peripheral lymphatic development. The fetal lymphatic morphology seems not to represent a mini-version of the adult morphology.
Key words D2-40 immunohistochemistry; human fetus; peripheral lymphatic vessels.

Introduction

Knowledge of the peripheral lymphatic anatomy in human fetuses has been very limited as most of the previous descriptions focused on the thoracic duct and major lymph trunks of early-stage fetuses (Sabin, 1909, 1912; van der Putte & van Limborgh, 1980; Petrenko & Gashev, 2008). However, to a greater or lesser extent, previous macroscopic descriptions of human lymphatics seem to have been based on injection studies using newborns and late-stage fetuses (e.g. Rouvière, 1981). Likewise, in Japan, in order to understand the 'adult' lymphatic morphology, many injection studies were previously performed using full-term fetuses (e.g. Inoue, 1936). From those studies, a concept emerged that lymphatic vessels (LVs) run along the artery and vein and connect between lymph node groups, and this became generally accepted for fetuses as well as adults. However, as lymph nodes develop later than LVs (Sabin, 1909, 1912; Bailey & Weiss, 1975), the pattern of fetal lymph follicle distribution is unlikely to determine the basic configuration of LV development.

The subcutaneous tissue and musculoskeletal system carry fewer lymph nodes than the viscera in spite of their large drainage areas. Wilting et al. (2003) hypothesized heterogeneous origins of lymphatic endothelial cells, i.e. the superficial LVs originate from the dermomyotome and the deep LVs from outgrowths of veins. If so, fetal LVs in the body wall and extremities are likely to display a configuration different from those of viscera although, even for adults, there is limited information about the subcutaneous tissue and musculoskeletal lymphatics (Pflug & Calnan, 1971; Suami et al. 2007). Against this background, we have questioned the accepted concept that fetal LVs develop or extend

Correspondence
Baik Hwan Cho, Department of Surgery, Chonbuk National University Medical School, San 2-20 Geumam-dong, Deokjin-gu, Jeonju, Jeonbuk 561-180, Korea. T: +82 63 250 1570; F: +82 63 271 6197; E: chobh@jbnu.ac.kr

Accepted for publication *26 February 2010*
Article published online *7 April 2010*

along the arteries and veins from deep areas to the superficial or peripheral parts of the body wall, extremities and subcutaneous tissues.

The intravisceral configuration of LVs has been well examined microscopically in the liver (Verbeke & Ruyssens, 1990; Ohtani & Ohtani, 2008a), heart (Landsberger & Heym, 1974; Okada et al. 2007), kidney (Ishikawa et al. 2006), pancreas (Krutikowa, 1970; O'Morchoe, 1997) and other organs (reviewed by Ohtani & Ohtani, 2008b). However, these studies included few observations of fetuses, especially human fetuses. Moreover, there seemed to be a 'gap' between the macroscopic and microscopic descriptions; for instance, there is little information on LVs in the mesentery and other supportive structures for the viscera. Do these visceral LVs run straight to a regional node, as demonstrated by injection studies? If the visceral or deep LVs are derived from outgrowths of veins, then fetal LV density is likely to be higher around the thoracic duct and several primitive lymphatic sprouts from deep veins (van der Putte & van Limborgh, 1980) than in the peripheral regions including each of the viscera.

Overall, we are sceptical that the fetal topographical anatomy of the lymphatics simply corresponds to a miniversion of the adult morphology. The aim of the present study was to describe the fetal morphology of the peripheral LVs using D2-40 immunohistochemistry in an 18-week female fetus and to evaluate the critical differences between the adult and fetal lymphatic morphologies. D2-40 or M2A is a good tool for the identification of peripheral LVs (Ishikawa et al. 2006; Yajin et al. 2009). It is also positive for some cells other than lymphatic epithelium such as in the nerve and gonad. However, the blood vessels are consistently negative. Because LVs do not accompany smooth muscles in mid-term fetuses (Jeong et al. 2009) and display a homogeneous architecture along their entire course from the periphery to their thoracic duct origin at 18 weeks of gestation, we did not discriminate the initial and collecting LVs, and referred to them as 'peripheral LVs' as a whole.

Materials and methods

The study was performed in accordance with the provisions of the Declaration of Helsinki 1995 (as revised in Edinburgh 2000). We examined an 18-week female fetus (CRL 155 mm). With agreement from the family, the specimen had been donated earlier to the Department of Anatomy, Chonbuk National University, Korea, and its use for research was approved by the university ethics committee. The fetus was obtained by induced abortion, after which the mother had been orally informed by an obstetrician (at a single hospital) about the possibility of donation for research; no attempt was made to actively encourage the donation. The mother subsequently agreed and the fetus was stored in 10% w/w formalin solution with an assigned specimen number for more than 3 months. Because of specimen number randomization, there was no possibility of contacting the family at a later date.

The whole fetus was divided into the head, cervical region, thorax, abdomen, pelvis and four extremities. After routine paraffin-embedding procedures for histology, 10-μm-thick sections were cut at 100-μm intervals; at least two adjacent sections were made at each slicing point. Horizontal sections were prepared for most of the regions but, for the cervical region, sagittal sections were made as another study on the fasciae had required them. Most sections were stained with hematoxylin and eosin, whereas the adjacent sections corresponding to one-fifth of almost 500 hematoxylin and eosin sections were subjected to immunohistochemistry to identify LVs. The number of sections used for immunohistochemistry was 95, including 15 for the cervical region, 15 for the thoracic region, 35 for the abdominal region, 20 for the pelvic region and 10 for the extremities. The primary antibody (monoclonal anti-human podoplanin; D2-40, Nichirei, Tokyo, Japan; 1 : 100 dilution) was used after immersion in a ligand activator (Histofine SAB-PO kit; Nichirei) with autoclave treatment (105 °C, 10 min). The secondary antibody (Chem Mate Envison kit; Dako, Glostrup, Denmark) was labeled with horseradish peroxidase and antigen–antibody reactions were detected via an HRP-catalysed reaction with diaminobenzidine. Counterstaining with hematoxylin was performed on the same samples.

To conventionally evaluate the numerical density, the numbers of intravisceral and subcutaneous LVs were counted in the highest-density area in the section at $\times$ 200 magnification using a $\times$ 20 objective lens. For one site or organ, we measured at least two sections after immunohistochemical staining. For visceral areas that were included in many sections, such as the jejunum and ileum, we used four to five sections for measurement. Not only cross-sections of LVs but also longitudinal sections were counted and included in the numbers. This method was based on Ishikawa et al. (2006).

Results

Figure 1 displays the orientation of major slices shown in the following figures of D2-40 immunohistochemistry. Another lower magnification view may also be helpful for the orientation (see Fig. 1 legend).

The density of D2-40-positive LVs was extremely high in the jugular node chain (Fig. 2) and axillary area (figure not shown), posterior mediastinum (Fig. 3), diaphragm (Fig. 4), mesentery of the small intestine (Figs 5 and 6), around the pelvic viscera (Fig. 7) and in the inguinal area (Fig. 8). The intervertebral foramen at any level of the vertebrae was one of the sites at which LVs were concentrated (Figs 2D and 4A). The intra- and perivisceral LVs showed appreciable differences in density between sites (Table 1). There were abundant LVs in and around the thyroid gland (Fig. 2A), lung (Fig. 3E), stomach (Figs 3A and 5D), small intestine (Fig. 5E), rectum (Fig. 7B) and pancreas (Fig. 5A–C). In contrast, no LVs were seen in the parathyroid gland (Fig. 2A), adrenal cortex (Fig. 6F) and spleen (figure not shown). The urogenital organs (Fig. 6A,C–E), colon (Fig. 6B), liver (Fig. 5F,G), larynx, pharynx, trachea (Figs 2B and 3D), esophagus (Figs 2B and 3D), thymus (Fig. 3F) and heart (Fig. 3C) displayed an intermediate LV density.

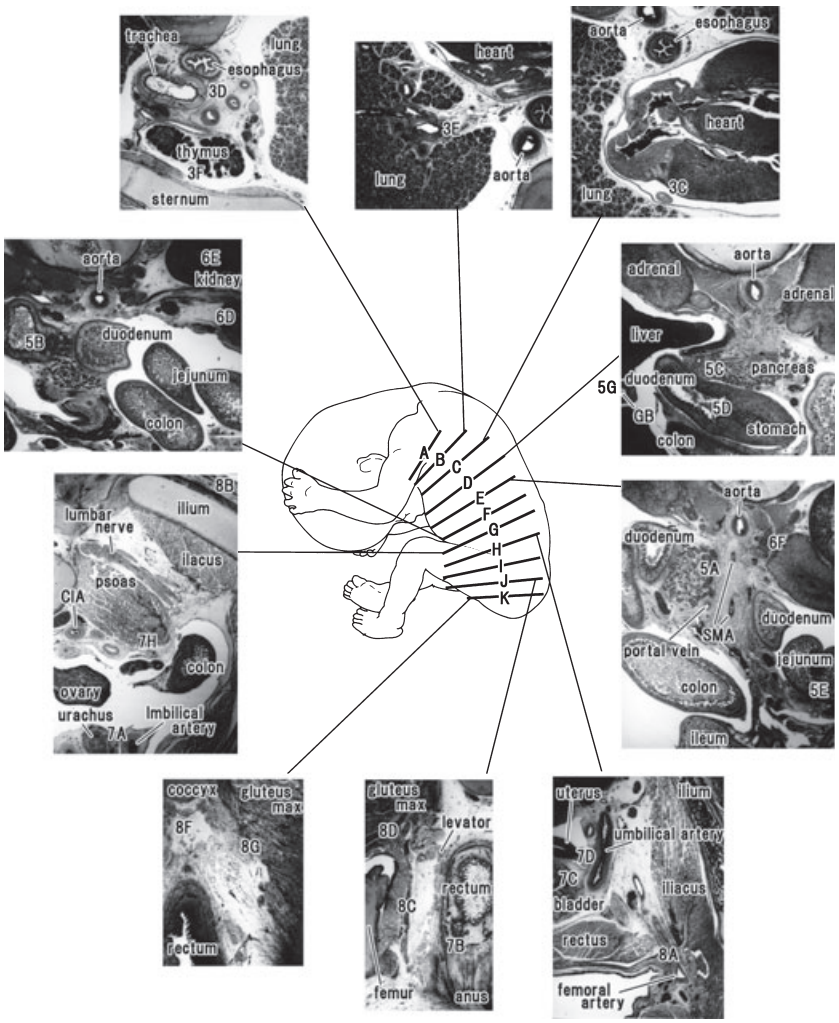

Fig. 1 Major slices shown in the following figures of D2-40 immunohistochemistry and their lower magnification views for orientation. A drawing of a fetus (center of the figure) is based on the observation of the fetus (CRL 155 mm) examined. Numbers with alphabetical characters, such as '3E' at level B, indicate the site shown in the following figure (e.g. Fig. 3E). Intervals of the levels A–K shown in the center of the figure do not correspond to the actual distances; they are 3.5 mm (between levels A and B), 11.7 mm (B and C), 26.1 mm (C and D), 3.2 mm (D and E), 5.8 mm (E and F), 13.1 mm (F and G), 5.4 mm (G and H), 9.2 mm (H and I), 5.0 mm (I and J) and 3.2 mm (J and K), respectively. Figure 3A,B displays a transition from the thoracic to abdominal regions hidden by the great interval between levels C and D. Figure 6A also explains a drastic change between levels F and G. CIA, common iliac artery; GB, gall bladder; gluteus max, gluteus maximus muscle; SMA, superior mesenteric artery.

In the thyroid (Fig. 2A), a loose network of LVs appeared to surround a cluster of follicles. The capsular LVs were also rich in the thyroid. In the thymus, specific vessels with cuboidal endothelium were weakly positive for D2-40 in the interstitium and capsule (Fig. 3F), possibly corresponding to the high endothelial venules, although developing lymph follicles did not yet contain such structures (Figs 2C, 5A, 6A, 8A,H). The hilar bronchi accompanied and contained abundant LVs (Fig. 3E) but, at the segmental level, LVs accompanied arteries rather than bronchi (figure not shown). Subpleural LVs were much fewer than LVs along the bronchial tree in the lung but the former were often dilated. Unexpectedly, in contrast to the intermuscular LVs, mucosal LVs of the esophagus were not identified by the present immunohistochemistry (Figs 2B and 3D). In the heart, LVs were not seen in the myocardium but were restricted to the loose tissue beneath the epicardium (Fig. 3C).

Subserosal LVs were greater in number than the mucosal, submucosal or intramural LVs in the stomach (Fig. 3A) but the relationship was reversed in the pylorus and small intestine (Figs 5D,E and 7B). The small intestine, i.e. the organ most likely to have the highest LV density, lacked most of the central LVs of the villi because of the time lag before fixation of the material (Fig. 5E). In the pancreatic parenchyma, LVs did not run along the ducts but ran indepen-

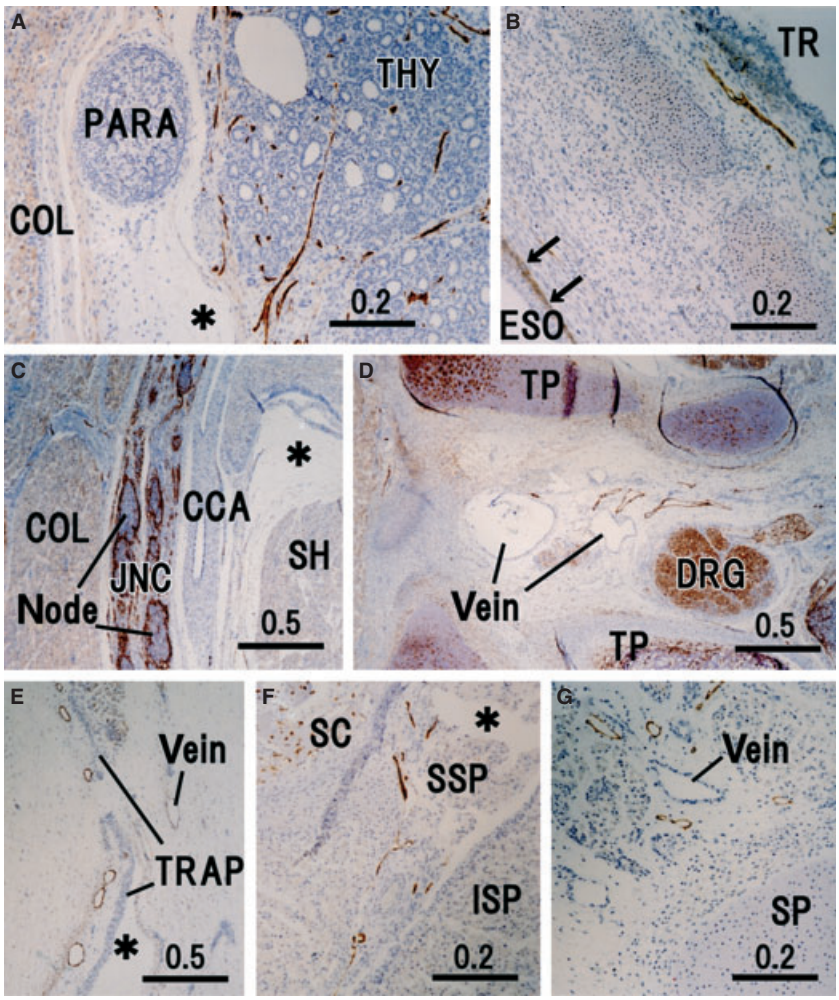

Fig. 2 Peripheral lymphatic vessels in the cervical region. Sagittal sections except for F and G. (A) Thyroid and parathyroid glands (THY and PARA) exhibiting well-developed lymphatic vessels (LVs) in the thyroid. (B) Trachea (TR) and cervical esophagus (ESO) containing positive immunoreactivity in the basal layer of the esophageal mucosa (arrows). (C) Jugular node chain (JNC) and common carotid artery (CCA). (D) LVs near the dorsal root ganglion (DRG) in a space between the transverse process (TP) of the sixth cervical vertebrae; the left-hand side (upside) of the panel corresponds to the dorsal side (superior side) of the body. (E) Superficial LVs along the broad rhomboidal aponeurosis of the trapezius (TRAP); the left-hand side (upside) of the panel corresponds to the superficial side (superior side) of the body. (F and G) Horizontal sections. (F) Border between the supraspinatus (SSP) and infraspinatus (ISP) exhibits a part of the lymphatic networks around the scapula (SC). (G) LVs near the spinous process (SP) of the cervical vertebrae. Asterisks in A, C, E and F indicate an artificial space during the histological procedure. COL, longus colli; SH, sternohyoideus.

dently in the interlobular connective tissue (Fig. 5C). Thus, there were no intralobular LVs in the pancreas. LVs along the surface of the pancreas were restricted to the head facing the great arteries (Fig. 5A) and near the common bile duct (Fig. 5B). Intramural LVs in the colon were fewer than in the rectum (Fig. 6B vs. 7B). The hepatoduodenal ligament contained abundant LVs. In the liver, LVs were still restricted to the area around the hilar thick portal veins (Fig. 5G) but they did not reach the segmental portal vein levels. In addition to the hilar region, LVs entered from the diaphragm into the liver near the inferior vena cava (figure not shown). The gallbladder bed contained abundant LVs running along the liver capsule (Fig. 5F). In addition, the renal capsule (Fig. 6D) and dura mater were strongly positive for D2-40, whereas the adrenal capsule was weakly positive (Fig. 6F).

The LVs ran circularly around the superior mesenteric artery and renal arteries rather than showing a straight course along them (Figs 5A and 6F). Thus, LVs appeared to provide a meshwork around these thick arteries. In contrast, LVs ran straight along the internal pudendal artery (Fig. 6C), inferior gluteal artery (Fig. 8D) and other middle-sized arteries to the body wall and extremities. The jugular node chain developed along and near the common carotid artery. However, it did not surround or even attach to the artery (Fig. 2C). The inguinal LVs were also separated from the femoral artery and vein (Fig. 8A).

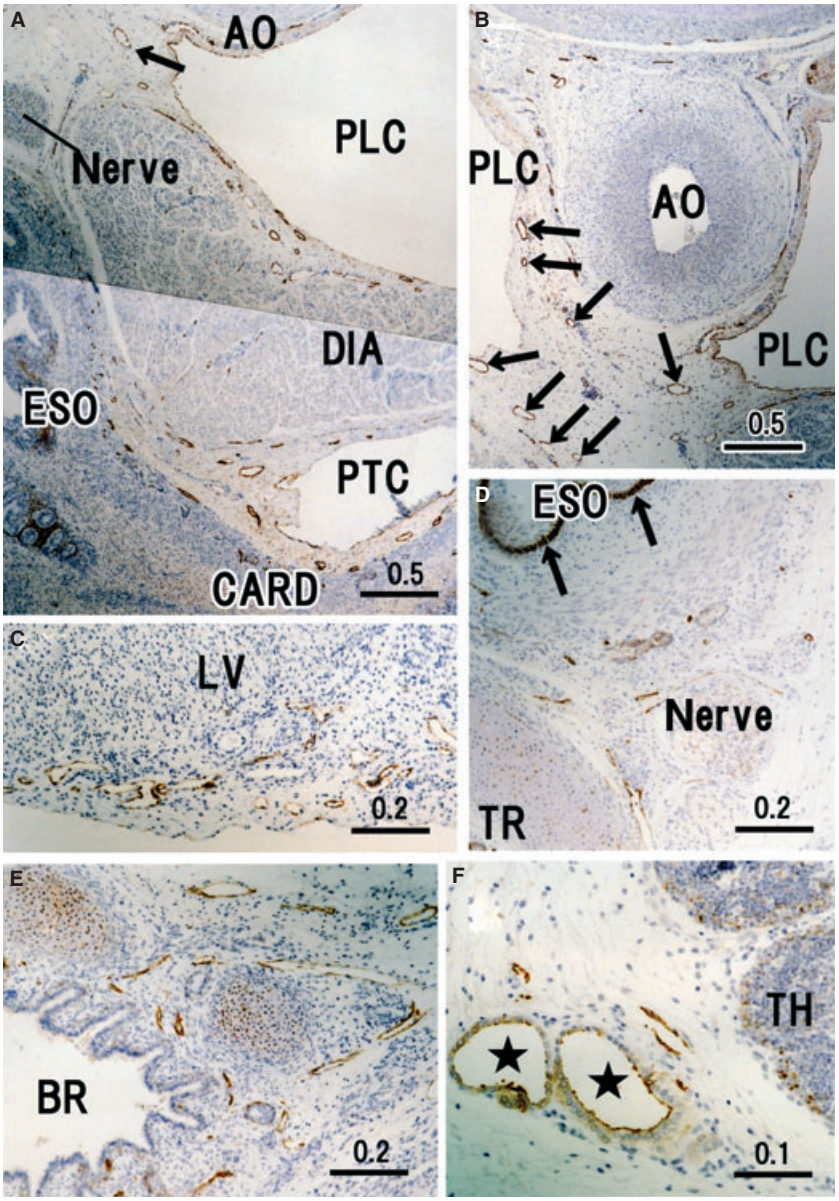

Fig. 3 Peripheral lymphatic vessels in and around the thoracic viscera. Horizontal sections. (A) Cardia of the stomach (CARD), abdominal esophagus (ESO), diaphragm (DIA) and aorta (AO) exhibit few lymphatic vessels (LVs) passing along the esophageal hiatus. (B) Dorsal side of A displays the thoracic duct tributaries (arrows), which originate from the abdomen. (C) LVs in the heart surface near the cardiac crux. LV, left ventricle. (D) Left angle between the trachea (TR) and thoracic esophagus (ESO) contains strongly positive immunoreactivity in the basal layer of the esophageal epithelium (arrows). (E) Left inferior lobar bronchus (BR) in the lung hilar region. (F) Capsule of the thymus (TH). Note two thick vessels comprising of cuboidal endothelium (stars). PTC, peritoneal cavity; PLC, pleural cavity;

The diaphragm contained abundant dilated LVs, especially in the pleural half of its thickness (Fig. 4E). Likewise, along the parietal pleura, the dorsal body wall carried thick LVs and received tributaries from the intervertebral foramen (Fig. 4A). At lateral and ventral sites, such as those along the costal pleura, LVs could not be identified with the present immunohistochemistry. In contrast, LVs beneath the parietal peritoneum were densely distributed in the ventral and lateral body wall (Figs 4D–G and 6A–C). In the lateral abdominal wall, the LVs ran in a space between the obliquus internus and transversus abdominis, and not between the obliquus internus and obliquus externus. Unexpectedly, a thick vessel corresponding to the thoracic duct was absent in the posterior mediastinum but several vessels of 0.1–0.2 mm in thickness ran in parallel in loose connective tissue between the aorta and esophagus (Fig. 3B).

There were abundant LVs along the scapula (Fig. 2F), spinous processes of the vertebrae (Fig. 2G), ribs (Fig. 4B) and coccyx (Fig. 8F) as well as dense connective tissues such as

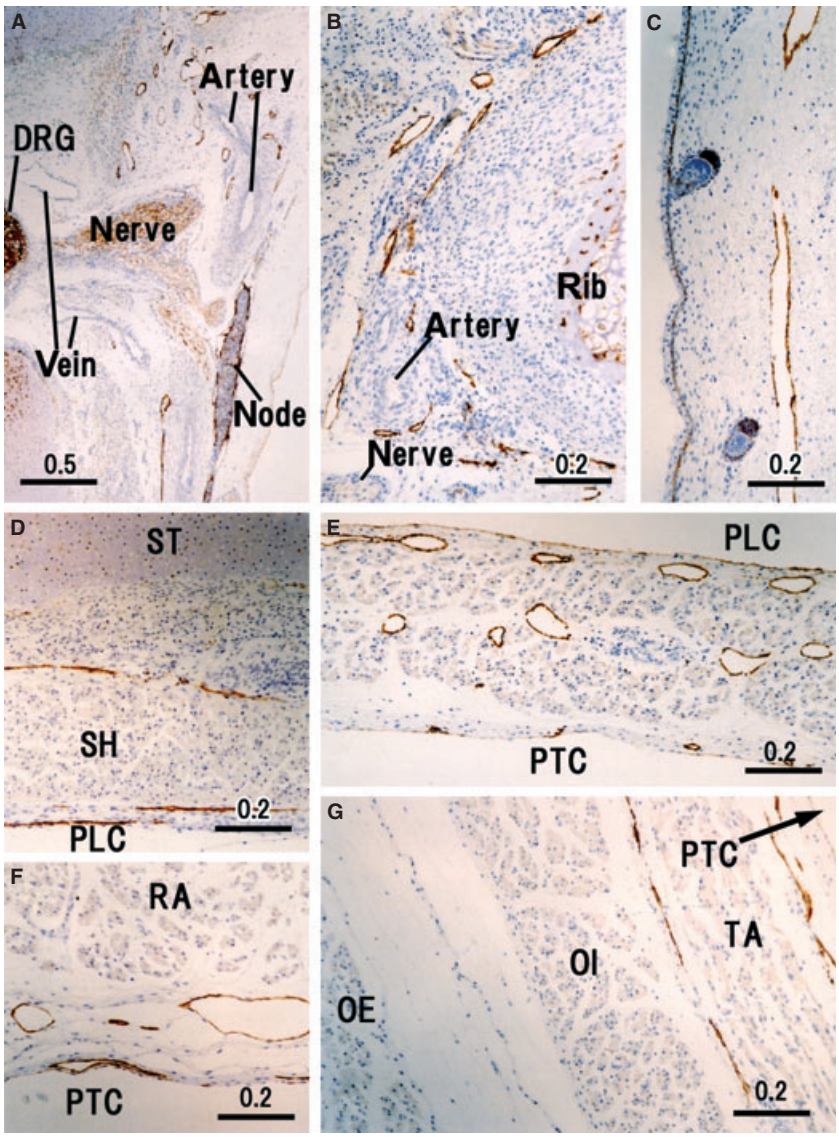

Fig. 4 Peripheral lymphatic vessels in the thoracoabdominal wall. Horizontal sections. (A) Dorsal root ganglion (DRG) and ventral nerve root (nerve) exhibit lymphatic vessels (LVs) along the pleural cavity (PLC). (B) LVs along the inferior edge of the rib. (C) Subcutaneous LVs in the lateral thoracic wall. (D) Ventral thoracic wall behind the sternum (ST) and sternohyoideus (SH). (E) Diaphragm containing abundant LVs; dilated LVs near the pleural cavity (PLC) and thin LVs along the peritoneal cavity (PTC). (F) Ventral abdominal wall behind the rectus abdominis (RA). (G) Lateral abdominal wall that is comprised of the obliquus externus (OE), obliquus internus (OI) and transversus abdominis (TA).

those along the pubic arch (Fig. 7I) and in the sacrotuberous ligament (Fig. 8G). Notably, LVs were not restricted to the inferior edge of the rib but were distributed evenly around the rib. No LVs were found in the intervertebral disk. A thick LV along the internal aspect of the psoas major (Fig. 7H) appeared to be a collateral of the external iliac chain of LVs. Lymph follicles were well developed in the popliteal fossa (Fig. 8H) and cubital fossa, in contrast to the situation in adults. In addition, lymph follicles were seen at two sites where nodes have not been reported previously in adults: (i) a connective tissue space along the superior gluteal artery running between the gluteus maximus and piriformis; and (ii) a connective tissue space along the obturator artery immediately outside the obturator membrane. The latter lymph follicle was located on the distal or upstream side of the LVs shown in Fig. 7E.

Subcutaneous LVs were diffusely distributed throughout the body and most of them were dilated. Their density did not differ markedly between subcutaneous areas (Table 1). All subcutaneous tissues were loose, irrespective of whether they were dense or loose in adults; typical areas corresponding to loose tissues in adults appeared in the lateral body wall (Fig. 4C), whereas areas corresponding to dense tissues in adults were present in the lateral aspect of the ilium

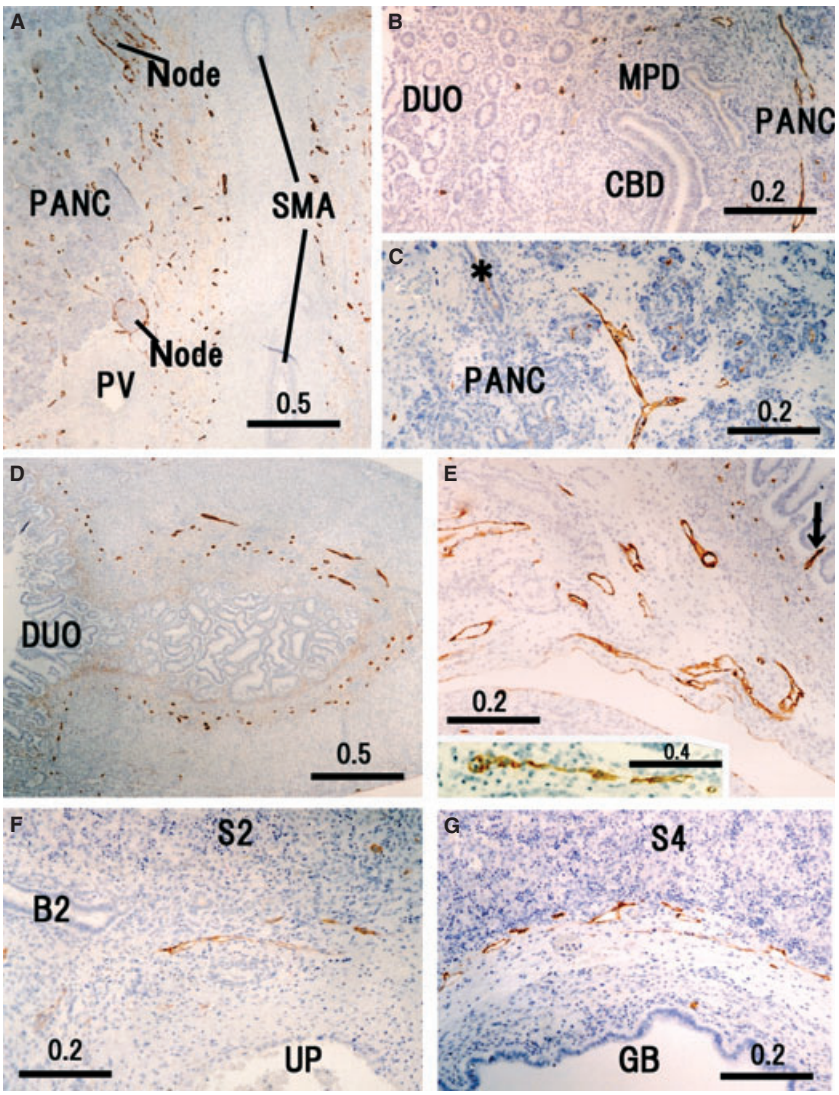

Fig. 5 Peripheral lymphatic vessels in and around the upper abdominal viscera. Horizontal sections. (A) Longitudinal section of the superior mesenteric artery (SMA) and the cross-section of the portal vein (PV) exhibits abundant lymphatic vessels (LVs) embedded in the nerve plexus along the artery. PANC, pancreatic parenchyma. (B) LVs around the Vater's papilla. CBD, common bile duct; DUO, duodenum; MPD, major pancreatic duct. (C) LVs separate from a pancreatic duct (asterisk). (D) Pylorus opening the duodenum (DUO). (E) Mesentery for the jejunum. A central lymph vessel (arrow) in an intestinal villus is seen at the right-hand side. An insert in E (the downside) shows another central vessel near E in the same section. (F) Umbilical portion (UP) of the left portal vein. (G) Bed for the gall bladder (GB). B2, segmental bile duct; S2 and S4, liver segments.

(Fig. 8B) and the dorsal aspect of the triangular aponeurosis of the trapezius (Fig. 2E). At the superficial aspect of the triangular aponeurotic origin of the trapezius, the subcutaneous LVs did not run along the craniocaudal axis but rather transversely. Perforating LVs connecting with deep LVs running along arteries and veins were few in number and they were not dilated.

Discussion

Although only a single fetal specimen was examined in this study, we demonstrated that the fetal lymphatic morphology differed from that in the adult in several points. Most of the differences seemed to be explained by the fact that fetal LVs were still increasing in number, density and areas of distribution. For example, the fetal renal LVs showed a distribution similar to that in adults (Ishikawa et al. 2006) but had a density 10–20 times lower. Another difference was the presence of two specific lymph follicles, one located along the superior gluteal artery and the other along the obturator artery. At these sites, to our knowledge, no nodes have been reported in adults. Thus, these follicles appear degenerate at later stages of development. However, no LVs were found in the spleen, parathyroid and adrenal

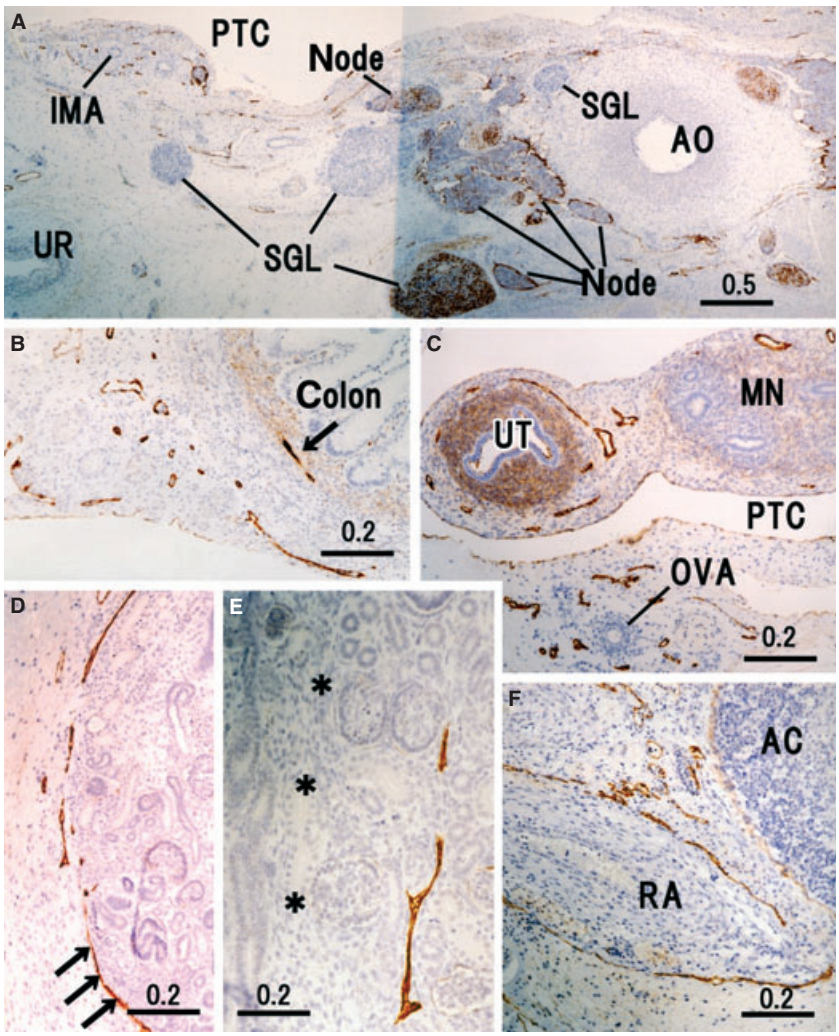

Fig. 6 Peripheral lymphatic vessels in and around the retroperitoneal viscera. Horizontal sections. (A) Aorta (AO), para-aortic nodes, inferior mesenteric artery (IMA) and ureter (UR). Abundant lymphatic vessels (LVs) run in the nerve plexus along these arteries. PTC, peritoneal cavity; SGL, sympathetic nerve ganglion. (B) LVs in the mesentery for the descending colon (colon) as well as a lymphatic vessel (arrow) in the colic wall. (C) Region around the uterine tube (UT) and ovarian artery (OVA). MN, mesonephros. (D) LVs running along the parenchymal margin at the renal hilus. (E) Lymphatic vessel in the cortex near the interlobar border (asterisks). Note, in D, that the renal capsule (arrows) is strongly positive for D2-40. In the left-hand side of E, longitudinally cut structures correspond to the proximal convoluted tubule. (F) LVs along the renal artery (RA); the adrenal cortex (AC) does not contain LVs but the capsule is weakly positive for D2-40.

gland. Thus, development of LVs in the fetus is unlikely to be simple (see below).

In the adult esophagus, the mucosal LVs are much more densely distributed than the submucosal and intermuscular LVs (Yajin et al. 2009). However, in contrast to the abdominal alimentary canal, the present fetal esophagus carried no mucosal LVs. Thus, in the esophagus, the mucosal LVs seemed to develop later than the intramuscular LVs. Likewise, the LVs beneath the epicardium seemed to develop earlier than those in the myocardium. Intrahepatic LVs also seemed to develop from the liver hilar region toward the segmental or subsegmental levels. However, another origin appeared likely at the LV-rich diaphragm around the hepatic vein terminals. In the pancreas, the interlobular LVs seemed to develop independently from the duct system and even independently from the arteries and veins, although, in newborns (Krutikowa, 1970), LVs densely surround all of the pancreatic acini.

The LVs in the diaphragm are well known to show a lattice-like configuration (Ohtani & Ohtani, 2008b). In the present case, the diaphragmatic LVs developed earlier on the peritoneal side than on the pleural side. A lattice-like configuration of LVs is also known to exist in the adult costal pleura (Masada et al. 1992, 1995; Ohtani & Ohtani, 2008a,b). However, the present subpleural LVs were restricted to the ventral and dorsal sites. The dorsal sub-

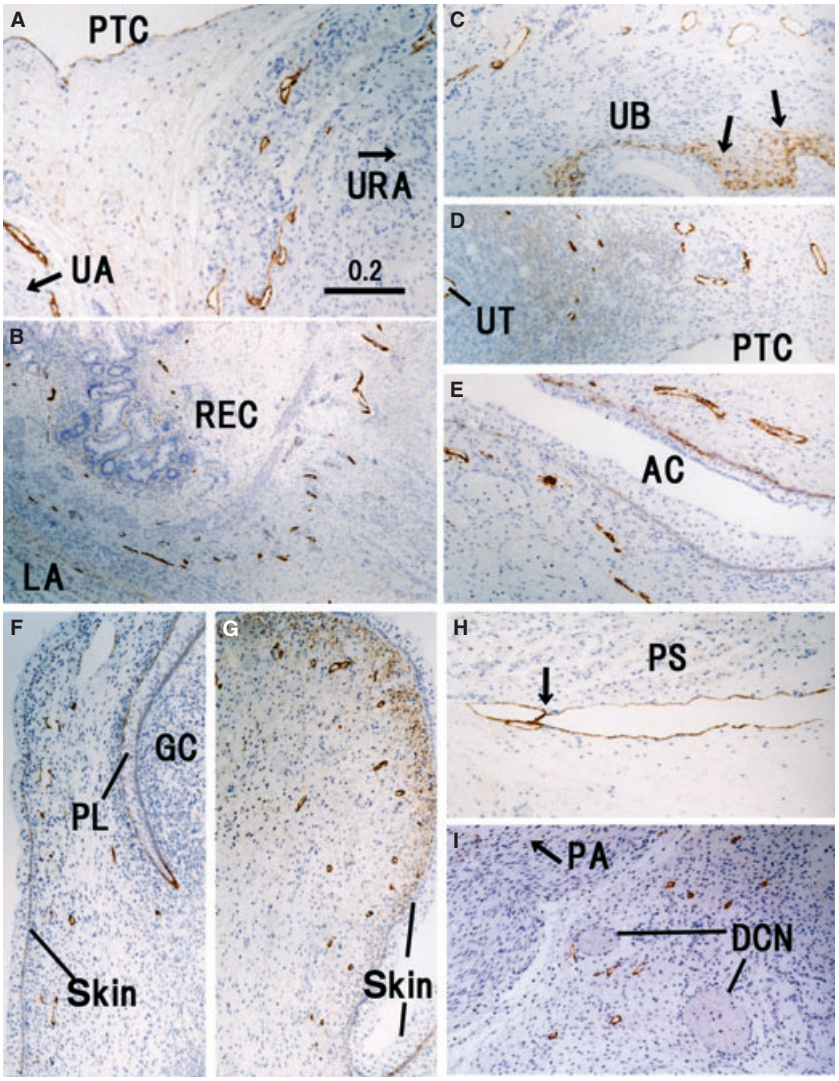

Fig. 7 Peripheral lymphatic vessels in and around the pelvic viscera. Horizontal sections. All panels are prepared at the same magnification (scale bar in A). (A) Lymphatic vessels (LVs) along the urachus (URA) and umbilical artery (UA). (B) LVs in the rectal wall (REC) attaching to the levator ani (LA). (C) Positive immunoreactivity in tissues around the urinary bladder (UB) as well as the basal layer of the epithelium (arrows). (D) LVs in the broad ligament of the uterus (UT). (E) LVs along the primitive anal cleft (AC). (F) Preputial lamella (PL) and glans of the clitoris (GC). (G) Subcutaneous tissue of the major labium. (H) Thick vessel along the internal surface of the psoas major (PS). Arrow indicates a candidate of the valve. (I) An area immediately below the bony pubic arch (PA). DCN, dorsal critoridis nerve; PTC, peritoneal cavity.

pleural LVs were likely to receive much lymph from the intervertebral foramen. The subpleural LVs behind the sternum might correspond to an example of the LV network around muscles and cartilages; such a network was evident around the scapulae and ribs. According to Gerecht-Nir et al. (2004), in the early stage, LVs tend to develop around the cartilages and primitive muscle masses. The present study also demonstrated that primitive ligaments contain abundant LVs. However, there is no information to indicate whether or not adult dense tissues, such as the sacrotuber ligament, contain abundant LVs.

The LVs crossed the superior mesenteric artery rather than running along it. Notably, these LVs passed through the tight autonomic nerve plexus. A meshwork of LVs was also evident around the other thick arteries (e.g. the renal artery). In contrast, the middle-sized arteries supplying the body wall and extremities had accompanying LVs running longitudinally along them. According to macroscopic observations (Deki & Sato, 1988; Ito et al. 1991), thin transverse LVs connect between thick upward LVs along the upper abdominal arteries. An almost straight course, as often seen in textbook figures (e.g. Rouvière, 1981), might have been overemphasized in injection studies. Surgeons believe that

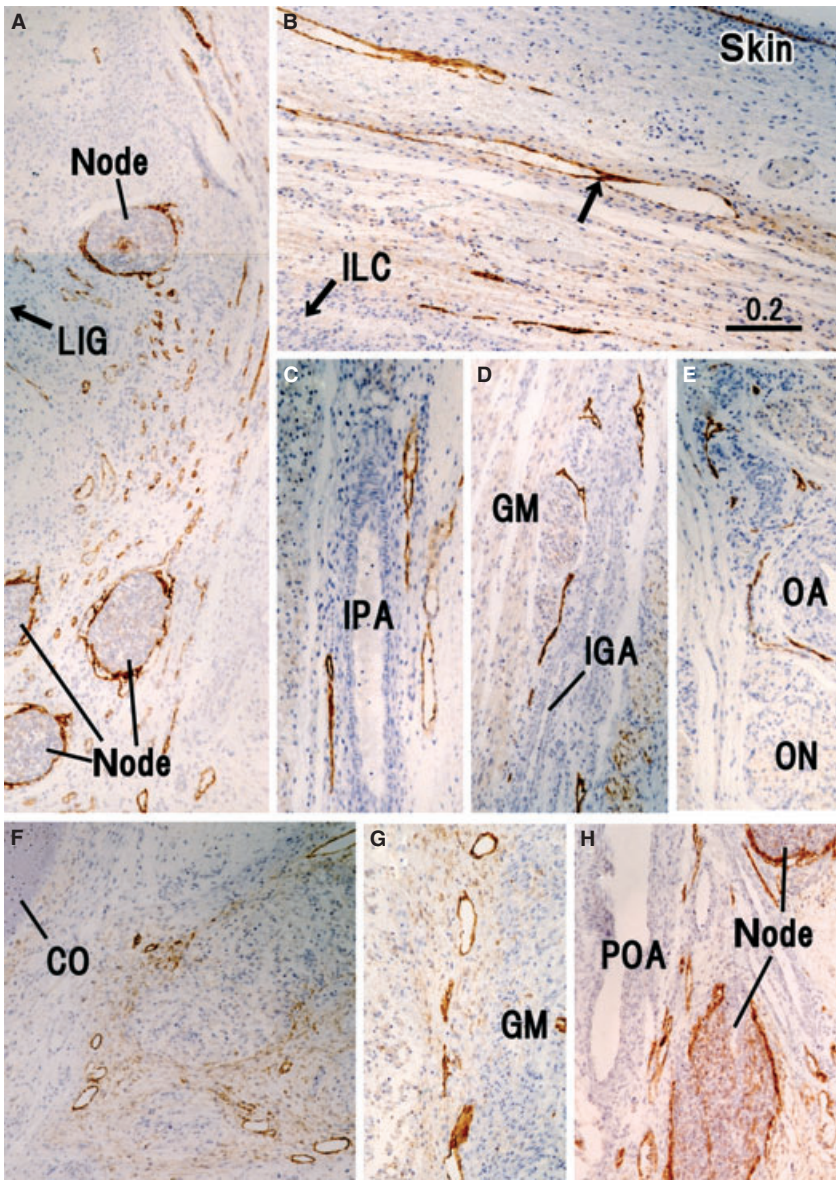

Fig. 8 Peripheral lymphatic vessels in the pelvic wall and inguinal region. Horizontal sections except for H. All panels are prepared at the same magnification (scale bar in B). (A) Lymphatic vessels (LVs) along the femoral canal beneath the inguinal ligament (LIG); the upside (or downside) of the panel corresponds to the internal (or femoral) side of the body. (B) Subcutaneous LVs in the lateral side of the iliac crest (ILC). Arrow indicates a candidate of the valve. (C) LVs along the internal pudendal artery (IPA) in the ischiorectal fossa. (D) Branch of the inferior gluteal artery (IGA) beneath the gluteus maximus (GM). (E) LVs along the obturator artery (OA) and nerve (ON) in the thigh. (F) LVs in front of the coccyx (CO). (G) LVs embedded in the developing sacrotuberal ligament. (H) Sagittal section; the downside of the panel corresponds to the inferior side of the extremity. LVs around the popliteal lymph follicles (node) and along the popliteal artery (POA) at the knee.

the upper abdominal nodes are located along arteries and/or veins (Japanese Research Society for Gastric Cancer, 1995; Japanese Pancreas Society, 1996). In mid-term fetuses, however, the upper abdominal LVs showed a strong tendency to run along the peritoneum or its remnant (i.e. the fusion fascia) in the common mesentery containing the celiac trunk and superior mesenteric artery. In contrast, outside the mesenteries, subperitoneal LVs were restricted to the ventral body wall near the umbilicus and urachus.

The subcutaneous LVs exhibited no clear site-dependent difference in density; they were diffusely distributed in all subcutaneous tissues in the body wall and extremities. Moreover, the subcutaneous LVs were often dilated. Such a superficial lymphatic morphology was in clear contrast to the deep LVs showing low density. As Wilting et al. (2003) considered (see Introduction), the deep LVs were unlikely to extend along the penetrating arteries and veins toward the subcutaneous tissue to provide an origin for subcutaneous

Table 1 Numbers of intravisceral and subcutaneous lymphatic vessels counted in the highest density area in the section under 20 × magnification field of objective lens (× 200).

Sites	Average	Range (difference between sections)
Thyroid, capsular and interfollicular	88	80–96
Parathyroid gland	0	0
Thymus	3	2–4
Trachea	10	9–11
Principal bronchus	23	21–25
Pulmonary hilum	8	6–10 (dilated)
Lung, peripheral parenchyma	13	11–15
Heart atrium, epicardium	12	9–18
Esophagus, intermuscular	12	8–14
Stomach (except for pylorus)*	10	8–12
Pylorus*	15	13–16
Duodenum*	13	10–18
Jejunum and ileum*	28	23–36
Colon*	10	6–17
Rectum	12	8–14
Hepatic hilum	17	15–19
Pancreas, parenchyma	12	9–15
Spleen	0	0
Kidney, interlobar	10	9–11
Urinary bladder, capsule	8	6–10
Ligamentum latum uteri	15	10–20
Subcutaneous area		
Back, thorax, abdomen	4	3–5 (dilated)
Lumbar, extremities	6	3–12

*Subperitoneal and intramural lymphatic vessels. Central lymph vessels of the intestine were excluded from the counting.

LVs. Simple sprouting from veins (van der Putte & van Limborgh, 1980; Karkkainen et al. 2003) seems insufficient to explain the fetal development of subcutaneous LVs. Ohtani and Ohtani (2008a) also hypothesized a dual origin of LVs in the fetal diaphragm. Prior to the formation of tubular vessels, numerous lymphatic endothelial cells independently migrate and then subsequently join together and connect with pre-existing LVs, thereby developing a lymphatic network.

Consequently, the fetal lymphatics do not represent a mini-version of the adult morphology as, at many sites, development appears to proceed in a step-by-step, and not a gradual, manner.

Acknowledgements

This study was supported by a grant (0620220-1) from the National R & D Program for Cancer Control, Ministry of Health & Welfare, Republic of Korea. We are grateful to Ms Masako Kuronuma (Yamagata University) for meticulous technical assistance for histology.

References

Bailey RP, Weiss L (1975) Ontogeny of the human fetal lymph nodes. *Am J Anat* **142**, 15–27.

Deki H, Sato T (1988) An anatomic study of the pancreatic lymphatics. *Surg Radiol Anat* **10**, 121–135.

Gerecht-Nir S, Osenberg S, Nevo O, et al. (2004) Vascular development in early human embryos and in teratomas derived from human embryonic stem cells. *Biol Reprod* **71**, 2029–2036.

Inoue Y (1936) Über das Lymphgefässyetem des Magens, Duodenums, Pankreas und des Zwerchfells. *Acta Anat Nippon* **9**, 35–117.

Ishikawa Y, Akasaka Y, Kiguchi H, et al. (2006) The human renal lymphatics under normal and pathological conditions. *Histopathology* **49**, 265–273.

Ito M, Mishima Y, Sato T (1991) An anatomical study of the lymphatic drainage of the gallbladder. *Surg Radiol Anat* **13**, 89–104.

Japanese Pancreas Society (1996) *Classification of Pancreatic Carcinoma*. 1st English edn. pp. 8–12. Tokyo: Kanehara.

Japanese Research Society for Gastric Cancer (1995) *Classification of Gastric Carcinoma*. 1st English edn. pp. 6–11. Tokyo: Kanehara.

Jeong YJ, Cho BH, Kinugasa Y, et al. (2009) Fetal topohistology of the mesocolon transversum with special reference to the fusion with other mesenteries and fasciae. *Clin Anat* **22**, 716–729.

Karkkainen MJ, Haaiko P, Sainio K, et al. (2003) Vascular endothelial growth factor C is required for sprouting of the first lymphatic vessels from embryonic veins. *Nature Immunol* **5**, 74–80.

Krutikowa IF (1970) Structure of interglandular vessels in the human pancreas. *Anat Anz* **127**, 189–199.

Landsberger A, Heym C (1974) Study of lymphatic vessels of the human heart. *Acta Anat* **89**, 149–160.

Masada S, Ichikawa S, Nakamura Y, et al. (1992) Structure and distribution of the lymphatic vessels in the parietal pleura of the monkey as studies by enzyme-histochemistry and by light and electron microscopy. *Arch Histol Cytol* **55**, 525–538.

Masada S, Nakamura Y, Nakamura H, et al. (1995) Distribution and structure of lymphatics in the human diaphragmatic and mediastinal pleura. *Haigan (Lung Cancer)* **35**, 875–882.

Ohtani O, Ohtani Y (2008a) Organization and developmental aspects of lymphatic vessels. *Arch Histol Cytol* **71**, 1–22.

Ohtani O, Ohtani Y (2008b) Lymphcirculation in the liver. *Anat Rec* **291**, 643–652.

Okada E, Akishima Y, Ito K, et al. (2007) Study on distribution of lymphatic vessels of the heart, and on lymphoangiogenesis in myocardium under myocardial infarction. An immunohistochemical study using D2-40 monoclonal antibody and anti-LYVE-1 antibody. *Jpn J Lymphology* **30**, 39–43.

O'Morchoe CC (1997) Lymphatic system of the pancreas. *Microsc Res Tech* **37**, 456–477.

Petrenko VM, Gashev AA (2008) Observations on the prenatal development of human lymphatic vessels with focus on basic structural elements of lymph flow. *Lymphat Res Biol* **6**, 89–95.

Pflug JJ, Calnan JS (1971) The normal anatomy of the lymphatic system in the human leg. *Br J Surg* **58**, 925–930.

van der Putte SC, van Limborgh J (1980) The embryonic development of the main lymphatics in man. *Acta Morphol Neerl-Scand* **18**, 323–335.

Rouvière H (1981) *Anatomie des Lymphatiques de L'Homme*. Paris: Masson.

Sabin FR (1909) The lymphatic system in human embryos, with a consideration of the morphology of the system as a whole. *Am J Anat* **9**, 43–91.

Sabin FR (1912) The development of the lymphatic system. In: *Manual of Human Embryology*, Vol. **2** (eds Keubel F, Mall FP, et al.), pp. 709–745, Philadelphia: Lippincott.

Suami H, Pan WR, Taylor GI (2007) Changes in the lymph structure of the upper limb after axillary dissection: radiographic and anatomical study in a human cadaver. *Plast Reconstr Surg* **120**, 982–991.

Verbeke C, Ruyssens N (1990) Intrahepatic lymphatics in the human fetus. *Lymphology* **23**, 36–38.

Wilting J, Tomarev SI, Christ B, et al. (2003) Lymphangioblasts in embryonic lymphangiogenesis. *Lymphat Res Biol* **1**, 33–40.

Yajin S, Murakami G, Takeuchi H, et al. (2009) The normal configuration and interindividual differences in intramural lymphatic vessels of the esophagus. *J Thoracic Cardiovasc Surg* **137**, 1029–1037.